Luminescence behaviour and deposition of Sc_2O_3 thin films from scandium(III) acetylacetonate at ambient pressure

Sebastian C. Dixon, Arreerat Jiamprasertboon, Claire J. Carmalt, and Ivan P. Parkin

Citation: Appl. Phys. Lett. **112**, 221902 (2018); doi: 10.1063/1.5038636
View online: https://doi.org/10.1063/1.5038636
View Table of Contents: http://aip.scitation.org/toc/apl/112/22
Published by the American Institute of Physics

Luminescence behaviour and deposition of Sc_2O_3 thin films from scandium(III) acetylacetonate at ambient pressure

Sebastian C. Dixon,[1] Arreerat Jiamprasertboon,[2] Claire J. Carmalt,[1] and Ivan P. Parkin[1,a)]
[1]*Materials Chemistry Centre, Department of Chemistry, University College London, 20 Gordon Street, London WC1H 0AJ, United Kingdom*
[2]*School of Chemistry, Institute of Science, Suranaree University of Technology, 111 University Avenue, Muang, Nakhon Ratchasima 30000, Thailand*

(Received 4 May 2018; accepted 17 May 2018; published online 30 May 2018)

Scandium(III) oxide thin film deposition has been historically difficult to achieve without the use of vacuum-based or wet chemical systems due to precursor limitations of low vapour pressure or ambient instability. In this letter, the adoption of aerosol-assisted delivery of scandium(III) acetylacetonate has enabled the chemical vapour deposition of polycrystalline and amorphous Sc_2O_3 thin films at ambient pressure with high growth rates (*ca.* 500 nm h^{-1}). The scandia films were intrinsically highly photoluminescent, exhibiting broad emission bands centred at 3.6 and 3.0 eV, which increased significantly in intensity upon aerobic annealing, accompanying a transition from amorphous to crystalline, while bands appearing at 2.1 and 2.3 eV seemed to occur only in the crystalline films. In addition, both amorphous and crystalline scandia films exhibited blue-green vibronic fine structure between 2.3 and 3.2 eV attributed to the electronic transition $B^2\Sigma^+ \rightarrow X^2\Sigma^+$ in surface $^{\cdots O-}_{\cdots O-}Sc = O$ groups and split by a vibrational mode observed at $920 \pm 60\,cm^{-1}$ by infrared spectroscopy. Band gaps of amorphous and crystalline Sc_2O_3 were determined to be 5.3 and 5.7 eV, respectively *via* diffuse reflectance. All films had high refractive indices, varying between 1.8 and 2.0 at 400 nm depending on film thickness and carrier gas used in the deposition; film thicknesses less than *ca.* 300 nm were observed to have a strong influence on the refractive index measured, while there was little variation for films thicker than this. The synthesis process itself is exceedingly low-cost and facile thus promising streamlined industrial scalability.
https://doi.org/10.1063/1.5038636

Scandium(III) oxide is an important material used in laser optical coatings owing to its robustness against physical damage, its wide optical band gap (*ca.* 6 eV), and its relatively high refractive index in the UV range (1.8–2.0),[1,2] as well as forming high reflective multi-layer or dielectric layers in the fabrication of capacitors and thin-film transistor (TFT) technology, themselves essential components in portable electronics in the ever-growing industry of smartphones, smartwatches, laptop computers, and the Internet of Things.[3] With smart device manufacture at historic highs and increasing exponentially still, there is a need to roll out ever-faster and more flexible means of optoelectronic thin film deposition over wider areas. While various means are used for the deposition of scandia films, the foremost methods are metal-organic chemical vapour deposition (MOCVD)[4,5] or magnetron sputtering,[3,6] both of which are vacuum deposition methods. Deposition at atmospheric pressure tends to offer superior growth rates to vacuum-based methods due to significantly higher mass transport of precursor to the substrate being intrinsic to the method.[7] By eliminating the need for expensive sputtering targets or reduced-pressure deposition environments, atmospheric-pressure deposition methods are readily scalable to wide-area substrates for mass device fabrication.[8] The difficulties of Sc_2O_3 deposition were described in detail by Leskelä *et al.*;[9] chemical vapour deposition (CVD) of scandia thin films at atmospheric pressure has hitherto been hindered by a lack of precursors with suitably high vapour pressure for vapour transport and film growth to be practical, but recent advances in the scalability of aerosol-assisted precursor delivery systems mean that industrial scalability of atmospheric-pressure chemical vapour deposition now simply requires that precursors are soluble in suitable solvents.[8] One favourite of the scientific community for chemical vapour deposition of scandia films has been the β-diketonate family of precursors and their various permutations of substituted derivatives, for their ambient stability and ease of preparation.[4] While much progress has been made in this field with regard to enhancing volatility and lowering the melting point, nothing so far has been practical for atmospheric-pressure deposition. By exploiting the solubility of scandium(III) β-diketonates, particularly the low-cost and readily-available scandium(III) acetylacetonate [also known commercially as scandium(III) 2,4-pentanedionate], aerosol-assisted chemical vapour deposition (AACVD) stands ready to enable scandia thin film CVD at atmospheric pressure.

In a typical experiment, a solution containing scandium (III) acetylacetonate hydrate (200 mg) in methanol (30 mL) was prepared with stirring for *ca.* 15 min. Aerosol-assisted chemical vapour deposition was carried out at 550 °C using a

a)Author to whom correspondence should be addressed: i.p.parkin@ucl.ac.uk, Tel.: +44 (0)20 7679 4669, Fax: +44 (0)20 769 7463

5% H_2/N_2 carrier gas flowing at 1.0 l min^{-1}, though other carrier gases were used where explicitly noted in this work. Details of the AACVD method have been reported by us previously.[10] Deposition in the presence of a small amount of hydrogen gas yielded dark, carbonaceous films with the greatest thickness and best coverage of the substrate with respect to deposition under nitrogen or air and were therefore used as the basis for this work. All films were strongly adhered to the substrate, resisting removal by Scotch tape or steel scalpel. The as-deposited films could then be rendered clear, colourless, transparent, and crystalline under annealing at 580 °C in air for 6 h. It is possible that the improved coverage is due to assistance provided by the H_2 in decomposing the hydrocarbon section of the scandium(III) acetylacetonate complex, while incomplete oxidation of this leaves a dark carbonaceous remainder. Indeed, previous researchers have likewise found scandium(III) β-diketonate precursors to have relatively low growth rates of the deposited film in the absence of a reactive gas.[11,12]

Scandium(III) 2,4-pentanedionate (acetylacetonate) hydrate was obtained from Alfa Aesar. Nitrogen (N_2, 99.99%), hydrogen (5% H_2/N_2), and compressed air carrier gases were obtained from British Oxygen Company. Methanol (99.5%) was obtained from Merck Millipore. All of the above were used as supplied. The float glass substrate ($50 \times 145 \times 4$ mm) with a 50 nm SiO_2 barrier layer was supplied by NSG Pilkington, Ltd. and cleaned with water and detergent, isopropyl alcohol, and then acetone before use.

X-ray diffractometry was carried out at a glancing angle ($\theta = 1.0°$) in air on a Bruker D8 Discover diffractometer using monochromatic Cu $K_{\alpha 1}$ and $K_{\alpha 2}$ radiation wavelengths of 1.54056 and 1.54439 Å respectively, at a voltage of 40 kV and a current of 40 mA. Diffraction was measured between angles $2\theta = 10$–$66°$. Angle-resolved X-ray photoelectron spectroscopy was conducted on a Thermo Scientific Theta Probe Mk. II spectrometer with monochromated Al K_α radiation, a dual beam charge compensation system and constant pass energy of 50 eV (spot size 400 μm). Survey scans were collected in the binding energy range of 0–1200 eV. Data were calibrated against C1s (284.5 eV) and fitted using CASA XPS software. Diffuse reflectance was recorded using a Shimadzu dual-beam spectrometer against a barium sulphate standard. Specular reflectance and refractive index calculations were carried out using a Filmetrics F20 spectral reflectance system against a Si wafer standard. Photoluminescence was performed using a Horiba FluoroMax-4 spectrometer fitted with a Xe light source and a monochromator set to emit excitation wavelengths of 150 nm.

The crystal structures of the scandia films were probed using X-ray diffractometry as shown in Fig. 1, which revealed that scandia films as-deposited under air exhibited distinct diffraction peaks, with deposition under N_2 yielding somewhat broader diffraction and deposition under 5% H_2/N_2 apparently yielding an amorphous film. All of the films exhibited a baseline of broad, shapeless diffraction indicative of a significant quantity of amorphous scandia present in each. Niinistö *et al.* found that the crystallinity of Sc_2O_3 fabricated *via* atomic layer epitaxy depends strongly upon the availability of oxygen in the deposition, with deposition under ozone (O_3) necessary to obtain significant crystallite

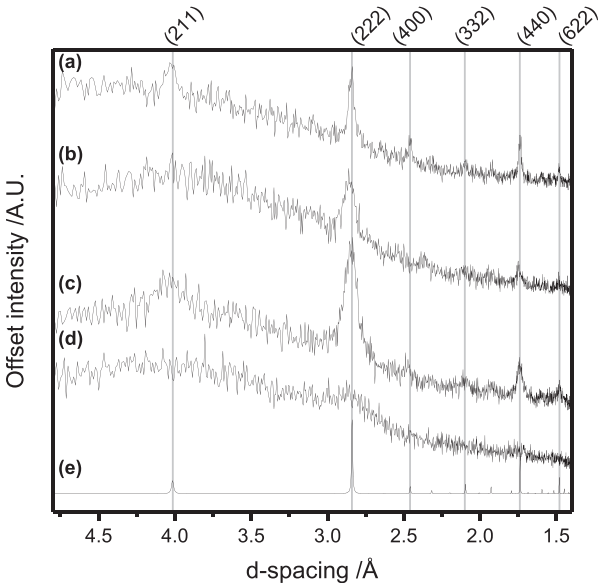

FIG. 1. X-ray diffractometry of scandia thin films, in the as-deposited state for deposition under (a) air, (b) N_2, (d) 5% H_2/N_2, and (c) the annealed state for the film deposited under 5% H_2/N_2, shown alongside (e) the Sc_2O_3 powder pattern (ICSD-26841).

growth.[12] This agrees well with the present observations, where moving through reducing, neutral then oxidising deposition environments delivers increasing crystallite growth in the as-deposited film. The fully amorphous film appeared to partially crystallise upon annealing with the characteristic Bragg peaks becoming strongly apparent, while in all cases, the (222) direction was clearly the preferred orientation, typical of scandia films.[11,12]

Photoluminescence under 150 nm irradiation of the scandia films deposited under hydrogen revealed a strongly luminescent behaviour, typical of scandium oxide.[13–16] The ratio of the instrument-corrected sample signal to the corrected reference beam is shown in Fig. 2(a). Many emission bands emerged in both films but more distinctly in the annealed film. Notably, the emission bands at 2.1 and 2.4 eV have been reported previously by Bordun and were attributed to radiative recombination of the excited donor-acceptor pairs in bonding orbitals between Sc^{3+} and adjacent O^{2-},[14] and were virtually absent in the amorphous films. Bordun argues that the rare earth sesquioxides Y_2O_3 and Sc_2O_3 are intrinsically fluorescent, owing not only to the behaviour of point defect states as is typical for many oxide systems[17,18] but also to the unique behaviour of donor-acceptor pairs in these materials.[14] That study used an excitation wavelength of 337.1 nm; however, by using a shorter excitation wavelength in the present work, it was possible to observe a further characteristic emission at 3.6 eV, more intense in the annealed film and having been previously ascribed to the emission of electrons trapped at oxygen vacancies (F-type centres),[13,15,16] though the enhancement in intensity of its emission upon aerobic annealing raises uncertainty over this assignment.

The occurrence of fine blue-green PL structure centred at between 2.5 and 3.2 eV in Fig. 2(a) is an indication of species with vibrational freedom. Previous work on yttria powders leads us to suggest that the vibrational quanta giving

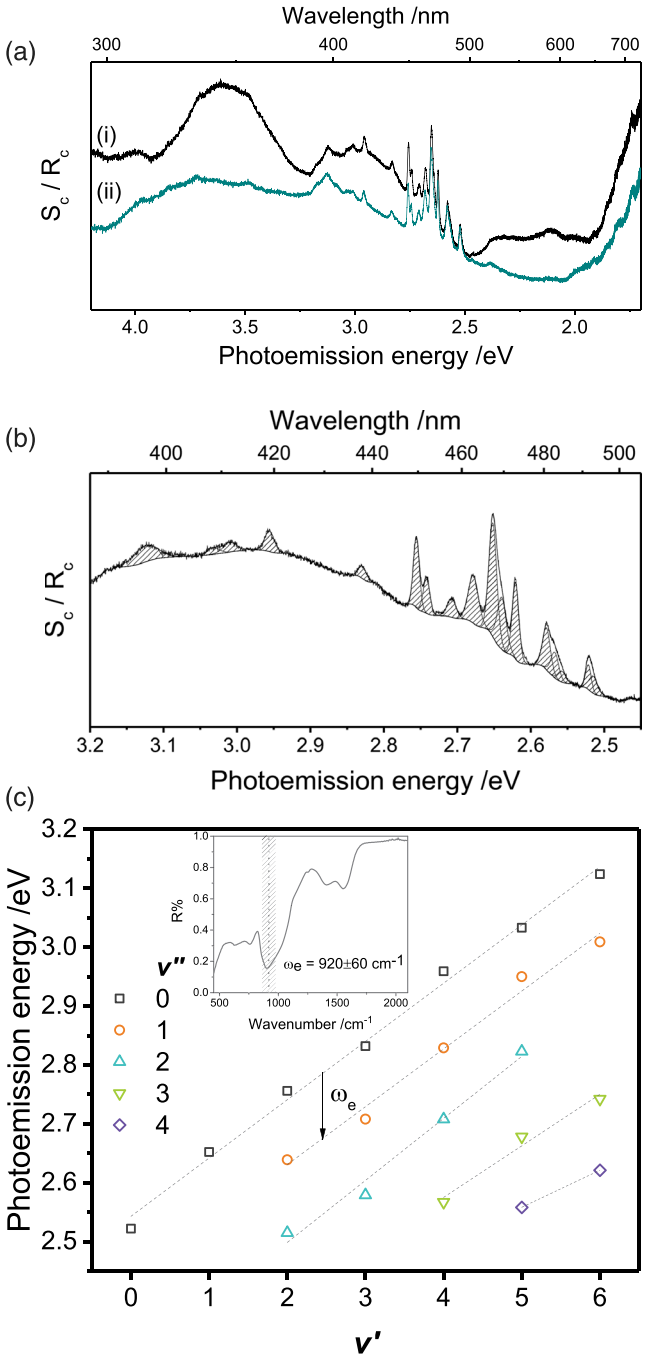

FIG. 2. (a) and (b) Photoluminescence (PL) spectra using excitation wavelength 150 nm (8.3 eV), where the ordinate axis represents the ratio of the instrument-corrected signal to the corrected reference beam, for [a(i)] as-deposited and [a(ii)] annealed Sc_2O_3 films. (b) The fitting of the vibronic splitting in the PL spectrum of the annealed Sc_2O_3 film is shown under closer focus. (c) The peak positions of the vibronic emissions are shown against their index assignments, where v' and v'' represent the vibrational quanta in the initial (excited) and final (ground) electronic states, respectively, with (*inset*) the corresponding vibrational absorption in the infrared reflectivity spectrum at 920 ± 60 cm^{-1}.

rise to the splitting within the ground and excited electronic states originate from surface-bound $^{\cdots O-}_{\cdots O-}Sc=O$ radical species,[13,19] a conclusion which is supported by the observation that these modes are distinctly present and unperturbed both before and after annealing and therefore independent of the bulk nature of the films. On the other hand, the lack of fine structure in the broad modes observed at 3.0 and 3.6 eV supports the conclusion that those modes arise in the bulk of the films, in which vibrational modes form a continuous series of minute vibrational quanta. The fine structure observed here has the greatest resolution obtained hitherto for $^{\cdots O-}_{\cdots O-}Sc=O$ bound radicals, enabling reliable deconvolution using Gaussian peak fittings as shown in Fig. 2(b) and arranged into vibronic transition series detailed in Fig. 2(c). A previous spectroscopic study on the $^{45}Sc^{16}O$ dimer indicates that these peaks correspond to the vibronic series $B^2\Sigma^+ \rightarrow X^2\Sigma^+$ where B and X are the excited and ground electronic states respectively, both with $^2\Sigma^+$ character, with the fundamental transition from $v'=0$ to $v''=0$ here at 2.52 eV (20 300 cm^{-1}), previously observed in the dimer at 2.55 eV (20 600 cm^{-1}).[20] Other previous works[21,22] enabled identification of various $v'=0, 1, 2, 3, 4$ to $v''=0, 1, 2$ transitions while the regular series spacings were used to expand the series assignment from the PL spectra here in order to obtain the set shown in Fig. 2(c). The mean separation and standard error of transitions to the $v''=0$ and $v''=1$ states were used to estimate the equilibrium vibrational frequency, and found to be $\omega_e = 110 \pm 10$ meV, which could be directly observed in the Fourier Transform Infrared spectroscopy reflectance spectrum at 920±60 cm^{-1}, shown in Fig. 2(c) (*inset*) while observed previously in the ScO diatomic molecule at 119.65 meV (964.95 cm^{-1}).[20]

Upon inspection of diffuse reflectance (DR) spectra of the as-deposited and annealed scandia films in Fig. 3, it is clear that the partial crystallisation of the amorphous Sc_2O_3 film by annealing has resulted in the appearance of a high-energy reflection maximum at 5.66 eV, denoted here as $R_{max,cryst.}$ and marked on the diffuse reflectance spectrum. This peak is absent in the amorphous film and therefore is likely due to the wider bandgap of the nascent crystalline phase. Since the occurrence of a broad diffraction "floor" in the XRD (Fig. 1) indicates only partial crystallisation, the appearance of the reflectance maximum $R_{max,amorph.}$ at *ca.* 5.23 eV in both the as-deposited and annealed films can be ascribed to the amorphous portion of the films. DR measurements close to these band gap absorption regions enabled estimation of their band gap widths by applying the method detailed by Murphy,[23] as shown in Eq. (1) where the absorption A is estimated by a point-by-point subtraction of the entire diffuse reflectance spectrum profile R_{diff} from the reflectance maximum R_{max} occurring at a nearby longer wavelength outside the reflectance trough corresponding to the band gap absorption, such that $A=0$ at R_{max}, as illustrated in Fig. 3. In this case, since there are two reflectance maxima at $R_{max,cryst.}$ and $R_{max,amorph.}$ corresponding to crystalline and amorphous portions of the partially crystallised film, respectively, A has been calculated using $R_{max,cryst.}$, which occurs at the higher reflectance of the two

$$A = R_{max} - R_{diff}. \quad (1)$$

From the absorption spectra, it is possible to estimate the band gap energies at the intersection of a linear fit to the absorption edge with a horizontal line drawn at the base of the local absorbance minimum. Applying this method, the bandgap of the as-deposited film had $E_{g,amorph.} = 5.3$ eV while the bandgap of the amorphous portion of the annealed film likewise had $E_{g,amorph.} = 5.3$ eV and the crystalline part

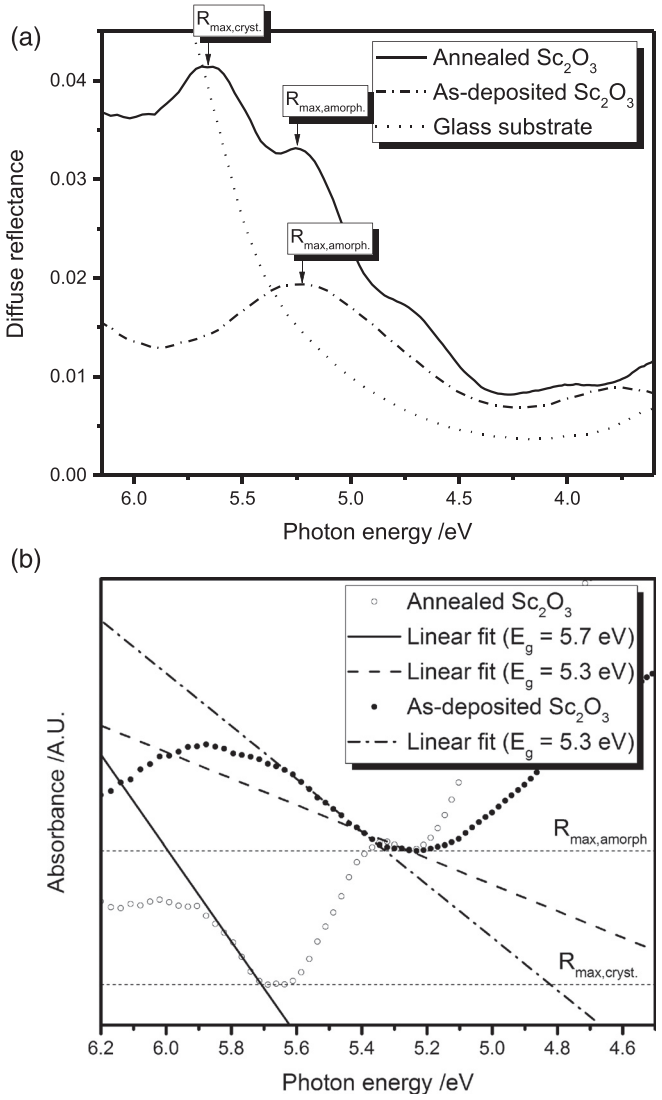

FIG. 3. (a) Diffuse reflectance spectra of scandia films as-deposited in the presence of H_2 and annealed, where $R_{max,amorph.}$ and $R_{max,cryst.}$ indicate the reflectance peaks used in the determination of band gaps for the amorphous and crystalline portions of the films, respectively, and (b) absorbance plots obtained thereafter with band gaps indicated.

had $E_{g,cryst.} = 5.7$ eV. While we ascribe this shift to crystallisation of the amorphous scandia, previous observers Shan *et al*. have noted that this may also arise due to concurrent elimination of intergap defect states upon aerobic annealing.[24]

Murphy warns that film densification under heat treatment affects an increase in the refractive index and therefore an increase in the apparent band gap when using the DR method;[23] however, this is not observed here as shown in Fig. 4(a), where it is evident that annealing actually affected a slight decrease in the refractive index profile. This is likely due to the fact that the annealing carried out here affected a phase transition from amorphous to crystalline, which was not accounted for in Murphy's discussion. Indeed, the amorphous film as-deposited in the presence of H_2 appeared to have one of the higher refractive index profiles as compared with the other, crystalline, samples. The effect of film thickness on the refractive index of the annealed scandia film deposited in the presence of H_2 is shown in Fig. 4(b), where it is apparent that thinner films seem to have lower refractive indices, due to an increased significance of the substrate-film interfacial region at lower thicknesses,[23] while above a thickness of *ca*. 300 nm, it seems that thickness variation has little effect on the refractive index. For this reason, films with thicknesses in the region of 350±20 nm were used for the comparison in Fig. 4(a), so that slight thickness variations between the films were less likely to influence their assessment.

X-ray photoelectron spectroscopy of the annealed film indicated, in the survey scan in Fig. 5(a), that the most significant contaminant in the scandia films other than C was Cl, though apparently only present in relatively minute quantities, below the quantification limit for a survey scan. It is unclear how adventitious Cl came to appear in these samples as all precursors involved in their deposition were nominally Cl-free; however, metal chlorides are common precursors in organometallic synthesis and it is likely that this impurity was present in the commercial $Sc(acac)_3$ precursor.

Angle-resolved XPS measurements (ARXPES) of the Sc 2p environment were undertaken to ascertain the shift in orbital energy levels close to the surface, as this is an important consideration in surface-dependent applications such as photoadsorption of gas molecules in photochemistry[25] or band offsets for gate dielectric applications.[3] Figures 5(c) and 5(d) illustrate the shift and broadening of the Sc $2p^1/_2$ and $^3/_2$ peaks, respectively. The angle shown describes the geometric relation between the sample and the photoelectron probe; a zero-degree angle indicates direct and perpendicular measurement (i.e., the deepest penetration) while a full 90° angle would imply a parallel or side-on scan. It can be seen that the binding energy of Sc 2p states in both cases is highest closest to the surface of the film, corresponding to XPS measured at high angles. Throughout the range measured, the binding energy of both orbitals shifted by *ca*. 0.1 eV, potentially a significant quantity where band offsets are concerned;[3] indeed, the position of the scandia valence band

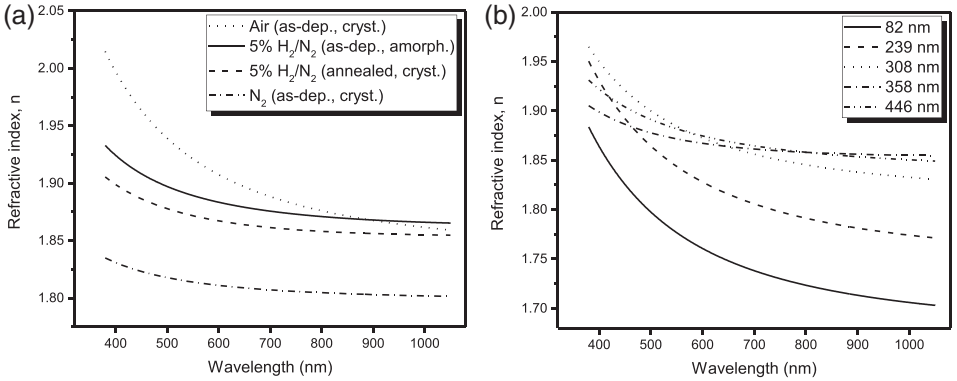

FIG. 4. Refractive index profiles calculated from specular reflectance of (a) 350 nm-thick (±20 nm) crystalline and amorphous films as-deposited under oxidising, neutral, and reducing carrier gases (with the exception of one annealed sample as shown), and (b) the effect of thickness on the refractive index of the annealed film deposited under 5% H_2/N_2.

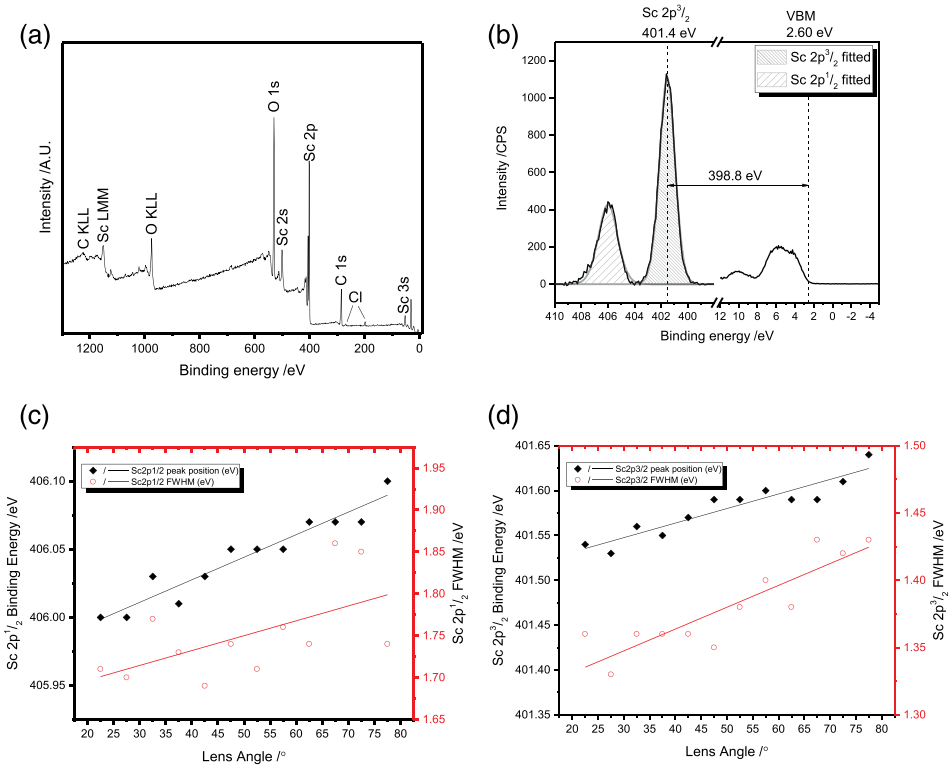

FIG. 5. X-ray photoelectron spectroscopy of annealed scandia films showing (a) representative survey spectrum, (b) separation of the Sc $2p^3/_2$ level from the valence band maximum, and Angle-resolved XPS measurements (ARXPES) of (c) Sc $2p^1/_2$, and (d) Sc $2p^3/_2$ peaks, respectively, illustrating peak shift to higher and broader binding energies as a function of photoelectron lens angle, inversely proportional to the depth probed beneath the surface.

maximum (VBM), given here in Fig. 5(b) as 2.60 eV, at the interface relative to a conducting substrate such as ZnO (whose VBM was found in previous work to be *ca.* 2.6 – 2.9 eV[3,10]) is key to the ability of scandia to act as a passivating or dielectric layer.

To summarise, chemical vapour deposition of scandia (Sc_2O_3) thin films has been achieved at atmospheric pressure using aerosol delivery of a solution containing scandium(III) acetylacetonate. Varying degrees of crystallinity of the deposited films could be achieved by varying the oxidising character of the deposition environment. The films exhibited physical properties typical of scandia, with wide band gaps of 5.3 and 5.7 eV corresponding to amorphous and crystalline scandia, respectively, and high refractive indices varying between *ca.* 1.8–2.0 at 400 nm depending on film thickness and deposition environment. The films exhibited strong photoluminescent character under UV irradiation, with broadband emission in amorphous scandia giving way to narrower bands in the crystalline film corresponding to well-known intrinsic bonding and defect-localised electron states. The presented fabrication method for scandia films is facile and readily scalable to industrial production.

NSG Pilkington Glass, Ltd., and the Engineering and Physical Sciences Research Council (EPSRC) are thanked for studentship funding (S. C. Dixon) through the UCL Molecular Modelling and Materials Science Doctoral Training Centre (Grant No. EP/G036675). Professor P. F. McMillan is thanked for helpful discussion of the photoluminescence series.

[1]Z. Xu, A. Daga, and H. Chen, Appl. Phys. Lett. **79**, 3782–3784 (2001).
[2]I. Ladany, P. J. Zanzucchi, J. T. Andrews, J. Kane, and E. DePiano, Appl. Opt. **25**, 472 (1986).
[3]D. C. Hays, B. P. Gila, S. J. Pearton, B.-J. Kim, F. Ren, and T. S. Jang, J. Vac. Sci. Technol., B: Nanotechnol. Microelectron.: Mater., Process., Meas., Phenom. **33**, 051218 (2015).
[4]K. V. Zherikova, L. N. Zelenina, T. P. Chusova, N. B. Morozova, S. V. Trubin, and E. S. Vikulova, Phys. Procedia **46**, 200–208 (2013).
[5]A. P. Milanov, K. Xu, S. Cwik, H. Parala, T. de los Arcos, H.-W. Becker, D. Rogalla, R. Cross, S. Paul, and A. Devi, Dalton Trans. **41**, 13936 (2012).
[6]A. Belosludtsev, K. Juškevičius, L. Ceizaris, R. Samuilovas, S. Stanionytė, V. Jasulaitienė, and S. Kičas, Appl. Surf. Sci. **427**, 312–318 (2018).
[7]S. C. Dixon, D. O. Scanlon, C. J. Carmalt, and I. P. Parkin, J. Mater. Chem. C **4**, 6946–6961 (2016).
[8]M. J. Powell, D. B. Potter, R. L. Wilson, J. A. Darr, I. P. Parkin, and C. J. Carmalt, Mater. Des. **129**, 116–124 (2017).
[9]M. Leskelä, K. Kukli, and M. Ritala, J. Alloys Compd. **418**, 27–34 (2006).
[10]S. C. Dixon, S. Sathasivam, B. A. D. Williamson, D. O. Scanlon, C. J. Carmalt, and I. P. Parkin, J. Mater. Chem. C **5**, 7585–7597 (2017).
[11]J. Selvakumar, V. S. Raghunathan, and K. S. Nagaraja, Chem. Vap. Deposition **15**, 262–268 (2009).
[12]M. Putkonen, M. Nieminen, J. Niinistö, L. Niinistö, and T. Sajavaara, Chem. Mater. **13**, 4701–4707 (2001).
[13]V. V. Solomonov, A. V. Spirina, A. V. Spirin, and S. N. Paranin, Opt. Spectrosc. **121**, 696–700 (2016).
[14]O. M. Bordun, J. Appl. Spectrosc. **68**, 304–307 (2001).
[15]A. V. Emeline, G. N. Kuzmin, D. Purevdorj, V. K. Ryabchuk, and N. Serpone, J. Phys. Chem. B **104**, 2989–2999 (2000).
[16]W. Hayes, M. J. Kane, O. Salminen, and A. I. Kuznetso, J. Phys. C: Solid State Phys. **17**, L383–L387 (1984).
[17]K. Ellmer and A. Bikowski, J. Phys. D: Appl. Phys. **49**, 413002 (2016).
[18]D. O. Scanlon and G. W. Watson, J. Mater. Chem. **22**, 25236 (2012).
[19]V. V. Osipov, A. V. Rasuleva, and V. I. Solomonov, Opt. Spectrosc. **105**, 524–530 (2008).
[20]K. P. Huber and G. Herzberg, *Constants of Diatomic Molecules* (Van Nostrand Reinhold, 1979).
[21]R. W. B. Pearse and A. G. Gaydon, *The Identification of Molecular Spectra*, 4th ed. (Chapman and Hall, London, 1976).
[22]W. F. Meggers and J. A. Wheeler, Bur. Stand. J. Res. **6**, 239 (1931).
[23]A. B. Murphy, Sol. Energy Mater. Sol. Cells **91**, 1326–1337 (2007).
[24]A. Liu, G. Liu, H. Zhu, H. Song, B. Shin, E. Fortunato, R. Martins, and F. Shan, Adv. Funct. Mater. **25**, 7180–7188 (2015).
[25]A. V. Emeline, S. V. Petrova, V. K. Ryabchuk, and N. Serpone, Chem. Mater. **10**, 3484–3491 (1998).